Development and characterization of nintedanib inhalable powders as a potential pulmonary fibrosis treatment

Valentina Ruggiero [a,b], Giovanna Aquino [a,b], Pasquale Del Gaudio [a], Teresa Mencherini [a], Consiglia Tedesco [c], Paola Russo [a,*]

[a] *Department of Pharmacy, University of Salerno, 84084, Fisciano, SA, Italy*
[b] *PhD Program in Drug Discovery and Development, University of Salerno, 84, Fisciano, SA, Italy*
[c] *Department of Chemistry and Biology "A. Zambelli", University of Salerno, 84084, Fisciano, SA, Italy*

ABSTRACT

Nintedanib is an orally administered intracellular tyrosine kinase inhibitor approved for idiopathic pulmonary fibrosis. Differently from oral treatment, dry powder inhalers (DPIs) can deliver a higher drug concentration at the target site, reducing doses and systemic side effects. The aim of this work was to develop dry powders of Nintedanib with properties suitable for inhalation therapy. Particles were prepared by spray drying the drug alone (3–5% w/v) or with appropriate excipients, from different hydroalcoholic solutions i.e., water/ethanol (7/3 v/v) or water/isopropyl alcohol (from 7/3 v/v to 5/5 v/v) mixtures. The powders obtained were characterized in terms of process yield, particle size distribution, morphology, density and aerodynamic properties. The results indicated that leucine improved the aerosol performance of the powders, increasing the value of the fine particle fraction (FPF) from 47.9 % in the drug only batches to 73.1 % using 5 % w/w leucine. This improvement was attributed to the ability of the amino acid to change both the surface area of the particles and the fluidity of the powder. Therefore, this study demonstrated the possibility of developing dry powder of Nintedanib for local administration in the lungs for the treatment of pulmonary fibrosis.

1. Introduction

Pulmonary fibrosis is a chronic and progressive disease characterized by the replacement of normal alveolar lung tissue with fibrotic tissue, resulting in irreversible impairment of respiratory functions [1]. Despite numerous treatments being explored in clinical studies, there are currently no effective preventive measures, largely due to a still limited understanding of the underlying pathogenetic mechanisms, especially in the idiopathic form known as idiopathic pulmonary fibrosis (IPF) [2]. The prevailing hypothesis suggests that IPF originates from repeated microscopic injuries to alveolar epithelial cells, followed by dysregulated repair. This process leads to uncontrolled proliferation of lung fibroblasts and differentiation into myofibroblasts, which excessively deposit extracellular matrix (ECM) in the interstitial space. Several profibrotic mediators, including platelet-derived growth factor (PDGF), fibroblast growth factor (FGF), and transforming growth factor-β, are believed to play a key role in the pathogenesis of IPF. Particularly, TGF-β1 acts in multiple ways: promoting chemotaxis and proliferation of fibroblasts, differentiation into myofibroblasts, production of profibrotic cytokines, and tissue inhibitors of metalloproteinases (TIMP), while inhibiting proteases involved in matrix degradation [3].

Nintedanib was one of the first drugs approved for the treatment of idiopathic pulmonary fibrosis (IPF) in the EU and USA (Varone et al., 2018). In 2019, it was further approved for the treatment of Systemic Sclerosis-Associated Interstitial Lung Disease (SSc-ILD), and in 2020, it was approved for Chronic Fibrosing Interstitial Lung Diseases with a Progressive Phenotype (Chronic Fibrosing ILD with a Progressive Phenotype) (Surber et al., 2020a). Recently, it was also proposed in the treatment of post-COVID-19 pulmonary fibrosis [4].

Specifically, Nintedanib is an intracellular inhibitor of tyrosine kinases, including platelet-derived growth factor, vascular endothelial growth factor, and fibroblast growth factor. Several preclinical studies report its interference with processes of active fibrosis, such as the proliferation and transformation of fibroblasts into collagen-producing myofibroblasts (Redente et al., 2018; Umemura et al., 2021 [3]). Oral administration of Nintedanib improves forced vital capacity and postpones disease progression, but only a small fraction of the orally administered drug reaches the epithelial airway surface (Andrade da Silva et al., 2023). Therefore, high and frequent dosages are required to achieve therapeutic efficacy in the lung, resulting in systemic side effects and economic burdens. Indeed, oral treatment is often associated with numerous gastrointestinal adverse events, leading to discontinuation of its use among patients with IPF (Fletcher et al., 2018; Ogura et al., 2015).

In this case, inhaled administration of the drug is favored (Eedara et al., 2021) due to its exclusive advantages, including a thin blood-alveolar barrier, large alveolar surface area, rapid clinical response, bypassing first-pass hepatic metabolism, high local concentration, and minimal systemic side effects [5]. Moreover, it offers patient compliance because it is a painless and non-invasive method compared to other routes, such as parenteral administration, resulting in improved therapeutic outcomes and a better quality of life for patients (Jain et al., 2020).

The development of an inhaled medicine that is effective and safe depends not only on the pharmacologically active molecule but also on the production of a respirable formulation and the selection of an appropriate device for its administration (Jain et al., 2020). In a recent study, nintedanib was reformulated as a solution for nebulization and direct inhalation administration to the lungs, demonstrating that very small inhaled doses are necessary to achieve an antifibrotic effect. This would also allow the dose to be increased for further efficacy while remaining below the oral systemic safety threshold (Surber et al., 2020b). In another study, fixed-dose combinations (i.e., two- and three-drug combinations) of Nintedanib, pirfenidone, and mycophenolic acid were produced and evaluated in dry powder for inhalation produced by thin-film freezing (TFF) (Praphawatvet et al., 2023). Kohei Togami et al. studied the antifibrotic effects of Nintedanib following its intra-pulmonary administration in a Nintedanib-CyD inclusion complex in mice with bleomycin-induced pulmonary fibrosis (Togami et al., 2022). As solid systems, dry powder inhalers (DPIs) have various inherent advantages, including higher stability, portability, and the capacity to deliver a higher drug concentration in the lung (Russo et al., 2012; Telko and Hickey, 2005; Gallo et al., 2019). Thus, the aim of this work was to develop dry powders of Nintedanib with physical and aerodynamic properties suitable for inhalation therapy using spray drying as a particle production technology. Indeed, this one-step technique allows the production of highly efficient inhalable particles, whose characteristics, including morphology, size, and density, can be tuned by optimizing the process parameters (Li et al., 2016a [6]). Different dry powder formulations were designed, and appropriate excipients were added to improve the technological properties of powders, including (LEU). This amino acid promotes good particle aerosolization by decreasing the surface energy (cohesive and adhesive forces) between particles, as it accumulates on the particle surface. It has also been shown that LEU (content greater than 20 % by weight) can recrystallize during spray drying by covering the particle surface and protecting it from moisture (Chvatal et al., 2019). To thoroughly study the ability to reach deep lung tissue, the influence of the feed compositions and operative conditions on the aerodynamic behavior and physicochemical characteristics of engineered particles were evaluated.

2. Materials and methods

2.1. Materials

Nintedanib was purchased from Hui Chem Co, Ltd (Shanghai, China). Sorbitan trioleate (span85), L-leucine, ethanol 96 % and isopropyl alcohol ≥99.8 % were provided from Sigma-Aldrich (Milan, Italy). Lecithin was obtained from Nutrition & Santè Italia S.p.A (Origgio, Italy). HCl 1 N was supplied from VWR Chemicals (Rosny-sous-Bois, France). Clear and colorless gelatine capsules size 3 were procured from Farmalabor (Canosa di Puglia, Italy). The inhaler device, Monodose DPI RS01 model 7, was kindly offered by Plastiape SPA (Lecco, Italy).

2.2. Powders preparation

Micronized particles were prepared (Table 1) by spray drying the drug alone or with a suitable excipient (span85, lecithin and L-leucine) from different hydroalcoholic solution i.e., water/ethanol (7/3 v/v) or water/isopropyl alcohol (from 7/3 v/v to 5/5 v/v) mixtures. The active

Table 1
Feed composition of spray-dried powders. Feed composition.

BATCH	H₂O/2-PrOH (v/v)	Total powder conc. (% w/v)	*Excipient (% w/w)		
			Span85	Lecithin	l-leucine
Niniso3	7/3	3	–	–	–
Niniso3	6/4	3	–	–	–
Niniso4	6/4	4	–	–	–
Niniso4	5/5	4	–	–	–
Niniso5	6/4	5	–	–	–
Niniso4_S85	6/4	4	1	–	–
Niniso4_le	6/4	4	–	1	–
Niniso4_leu10	6/4	4	–	–	10
Niniso4_leu7.5	5/5	4	–	–	7.5
Niniso4_leu5	6/4	4	–	–	5
Niniso4_leu5	5/5	4	–	–	5
Niniso4_leu2.5	5/5	4	–	–	2.5
Niniso5_leu10	6/4	5	–	–	10
Niniso5_leu5	6/4	5	–	–	5
Niniso5_leu5	5/5	5	–	–	5

ingredient (3–5% w/v) and span85 (1 % w/w) were both dispersed in alcohol, while L-leucine (from 2.5 % to 10 % w/w) and lecithin (1 % w/w) were dissolved in distilled water until complete solubilization, then the aqueous and the organic solvent were mixed under continuous magnetic stirring. The total powder concentration was between 3 % and 5 % w/v. In order to improve the drug solubility, each single feed was obtained by gradually adding few drops of 1 M hydrochloric acid solution up to pH 6 ± 0.5. Finally, the feed solution were dried using a Buchi mini spray dryer B-290 (Buchi Laboratoriums-Tecnik, Flawil, Switzerland) under the following operative conditions: inlet temperature 90 °C for batches with 30 % and 40 % v/v of isopropyl alcohol and ethanol, and 85 °C for batches containing 50 % v/v of isopropyl alcohol, drying air flow 500 L/min, aspiration rate 100 %, air pressure 7 atm, feed rate 5 ml/min and nozzle diameter 0.5 mm. The outlet temperature ranged between 53 °C and 58 °C depending on liquid feeds composition and inlet temperature. All the spray-dried powders were collected and stored at room temperature. Production yields were expressed as weight percentage of the final product compared to total amount of the material sprayed.

2.3. Powders physico-chemical properties

2.3.1. Nintedanib quantification

For drug content evaluation in spray-dried powders and for *in vitro* aerodynamic studies, Nintedanib was quantified by UV detection (Evolution 201, Thermo Fisher Scientific, Spectral, Ozzano dell'Emilia, Bologna, Italy) at a wavelength of 389 nm, using 1 cm SUPRASIL® quartz cell (Hellma 100-QS, HELLMA Italia srl, Milan, I). The analytic method was validated using standard solutions of Nintedanib in the range of 2–15 µg/ml ($y = 0.0546x + 0.0034$; $R^2 = 0.9985$; LOD 0.60 µg/ml; LOQ 1.81 µg/ml) using water and ethanol in a 7/3 ratio as solvent. For dissolution studies, the analytic method was validated using standard solutions of Nintedanib in the range of 2.58–17.2 µg/ml ($y = 0.055x + 0.0157$; $R^2 = 0.9995$; LOD 0.41 µg/ml; LOQ 1.23 µg/ml) using PBS and isopropyl alcohol in a 7/3 ratio as solvent.

2.3.2. Particle size

The particle size distribution of microparticles was determined using a light-scattering laser granulometer equipped with a tornado powder dispersing system (LS 13 320 Beckman Coulter Inc., FL, USA). The LS 13 320 uses a 5 mW laser diode with a wavelength of 750 nm and reverse Fourier optics incorporated in a fibre optic spatial filter and binocular lens systems. The particle size distributions were calculated by the instrument software using a *Fraunhofer Model*. The tornado module leads

to a dispersion similar to the one achieved when the samples are run wet, without using any solvent which can alter powder surface properties [7]. Samples were charged into a plastic cylinder to obtain an obscuration value between 4 and 8 %.

Results were expressed as d_{50} and span, defined as $[d(90) - d(10)]/d(50)$, where $d(10)$, $d(50)$ and $d(90)$ indicate diameters at the 10th, 50th and 90th percentiles of the particle size distribution, respectively.

2.3.3. Microparticle morphology

Morphology of microparticles was examined using a scanning electron microscope (SEM) Zeiss EVO MA10 with a secondary electron detector (Carl Zeiss SMT AG, München-Hallbergmoos, Germany), operating at 14 kV, equipped with a Leica EMSCD005 metallizator producing a deposition of a 200–440 Å thick gold layer [8].

2.3.4. Bulk and tapped density and Carr's index

Bulk density (ρ_b) and tapped density (ρ_t) of the spray-dried powders were measured as described elsewhere [9]. Briefly, powders were loaded into a bottom-sealed 1 ml plastic syringe (Terumo Europe, Leuven, Belgium) capped with laboratory film (Parafilm® "M", Pechiney Plastic Packaging, Chicago, IL, USA) and tapped on a hard bench until no change in the volume of the powder was observed. The bulk and tapped densities were calculated from the net weight of the plastic syringe content divided by the powder volume in the syringe before and after tapping, respectively. Carr's Index was defined as Eq.:

$$Carr's\ Index(\%) = \frac{(\rho t - \rho b)}{\rho t} \times 100$$

Experiments were performed in triplicate.

2.3.5. Differential scanning calorimetry (DSC)

Differential scanning calorimetry (DSC) was performed with an Indium-calibrated Mettler Toledo DSC 822e (Mettler Toledo, OH, USA). Accurately weighed samples (4–5 mg) (MTS Mettler Toledo microbalance, OH, USA) were placed in a 40 μL aluminium pan, which was sealed, pierced, and heated up to 350 °C at a heating rate of 10 °C/min.

2.3.6. Thermogravimetric analysis

Thermogravimetric analysis (TGA) was performed on the batches in a thermogravimetric analyzer (TGA Q5000, TA instruments, USA) in order to determine the amount of residual water in spray-dried powders. Six to 8 mg of sample were placed on a platinum pan. The pan was heated up to 300 °C in steps of 10 °C, under dynamic flow of dry nitrogen (200 mL/min).

2.4. Aerodynamic behavior evaluation

The aerodynamic properties of the powders produced were evaluated *in vitro* using the Single Stage Glass Impinger (SSGI apparatus, apparatus A Eur. Ph. 6.0, Copley Scientific Ltd., Nottingham, UK) and Andersen cascade impactor (apparatus D, European Pharmacopoeia 6.0, ACI, Westech Instrument Services Ltd., Bedfordshire, UK) and the monodose DPI RS01 model 7, a breath activated and reusable DPI.

For the experiments, 30 ml and 7 ml of hydroalcoholic solution (water/ethanol 7/3 v/v), were introduced in the lower and upper stages of the SSGI, respectively. Clear and colorless gelatine capsules (size 3) were filled manually with 30.0 (±0.5) mg of spray-dried powder. The capsule was horizontally inserted into the pulverization chamber and pierced twice: the inhaled air creates a turbulence that shakes and twists the capsule, facilitating its empty. The vacuum pump was operated at a flow rate of 60 ± 0.5 L/min for 5 s (Erweka vacuum pump VP 1000 equipped with an electronic digital flowmeter type DFM, Erweka Italia, Seveso, MI, Italy). Each deposition experiment was performed on 10 capsules. Upper and lower parts were washed with hydroalcoholic solution (water/ethanol 7/3 v/v) to recover the powder deposited on each stage and quantify the drug content by UV measurements. The emitted

dose (ED) was gravimetrically determined and expressed as percentage of powder exiting the device *vs* amount of powder introduced into the capsule. The Fine Particle Fraction (FPF), expressed as a percentage, was defined as ratio of the drug characterized by particles with an aerodynamic diameter smaller than 6.4 μm which passed into the lower impingement chamber *vs* total drug charged into the capsules.

The powders showing promising aerosolization properties were also tested with an Andersen cascade impactor modified for use at a flow rate of 60 ± 0.5 L/min and 30 ± 0.5 L/min. In this study, a flow rate of 60 L/min was chosen, since patients in the early phase of idiopathic pulmonary fibrosis (IPF) may have a relatively strong respiratory capacity. However, the respiratory capacity of patients with IPF tends to gradually decrease as the disease progresses [10]. In this regard, deposition studies were repeated using the Andersen cascade impactor by lowering the flow rate to 30 ± 0.5 L/min. To minimize particle bounce, metal impaction plates were dipped into an *n*-hexane solution of SPAN 80 (0.1 %, w/v) and the solvent was allowed to evaporate, leaving a thin film of SPAN 80 on the plate surface. The ACI was assembled placing a filter paper on the filter and the device was fitted into a rubber mouthpiece attached to the throat. The vacuum pump was actuated for 5 s. The powder deposited into the different stages was recovered by plunging each plate and the stage below in hydroalcoholic solution (water/ethanol 7/3 v/v, 25–250 mL depending on the number of stages). Drug content was assessed by UV measurements and the emitted dose (ED) was determined as described above for SSGI experiments. The cumulative mass of powders with a diameter lower than the stated size of each stage was calculated and plotted as a percentage of recovered powder *vs* cut-off diameter. The mass median aerodynamic diameter (MMAD) of the particles was extrapolated from the graph, according to the European Pharmacopoeia 6.0. From the same plot, the fine particle dose (FPD), i.e. the mass of Nintedanib with a particle size less than 5 μm, and the fine particle fraction (FPF), i.e. the fraction of Nintedanib emitted from the device with a particle size less than 5 μm, were determined (European Pharmacopoeia 6.0).

In vitro deposition experiments were performed on three batches with three replicates each.

2.5. Chromatographic conditions

RP-UHPLC-PDA analyses were performed on a Shimadzu Nexera UHPLC system (Kyoto, Japan) consisting of a SIL-30AC autosampler, a CBM-20A controller, a DGU-20A$_{5R}$ degasser, two LC-30AD pumps, a CTO-20AC column oven and, a SPD-M20A photodiode array detector.

For RP-UHPLC-PDA analyses a Kinetex® C18 150 × 2.1 mm (100 Å), packed with 2.6 μm core-shell particles column with a guard cartridge system (Phenomenex, Bologna, Italy) was employed at a flow rate of 0.4 mL/min. The mobile phase consisted of H_2O (A) and ACN (B), both acidified by HCOOH 0.1 % v/v. The analysis was performed in gradient elution as follows: 0.01–2.00 min, isocratic to 5 % B; 2.01–20.00 min, 5–95 % B; 20.01–23.00 min, isocratic to 95 % B; returning to initial conditions in 2 min; then 5 min for column re-equilibration. The following PDA parameters were applied: sampling rate, 12.5 Hz; detector time constant, 0.240 s; and cell temperature, 40 °C. Data acquisition was set in the range 190–400 nm, and chromatograms were monitored at 280 nm at maximum absorbance of the compounds of interest. Column oven was set to 40 °C. 3 μL were injected.

2.6. UHPLC-HRMS/MS conditions

UHPLC-HRMS/MS analysis was performed on a Thermo Ultimate RS 3000 coupled online to a Q-Exactive hybrid quadrupole Orbitrap mass spectrometer (Thermo Fisher Scientific, Bremen, Germany) equipped with a heated electrospray ionization probe (HESI II).

The ESI was operated in positive. The MS was calibrated by Thermo calmix Pierce™ calibration solutions in both polarities. Full MS (100–1500 *m/z*) and data-dependent MS/MS were performed at a

resolution of 35 000 and 17 500 FWHM respectively, normalized collision energy (NCE) values of 15, 20, and 25 were used. Source parameters: Sheath gas pressure, 50 arbitrary units; auxiliary gas flow, 13 arbitrary units; spray voltage, +3.5 kV, −2.8 kV; capillary temperature, 310 °C; auxiliary gas heater temperature, 300 °C.

Data analysis and processing were performed using FreeStyle™ 1.8 SP2 and the commercial software Compound Discoverer v. 3.3.1.111 SP1 (Thermo Fisher Scientific, Bremen, Germany).

2.7. In vitro dissolution study

Dissolution assays were performed by means of Franz-type vertical diffusion cells (Hanson research corporation, CA, USA).

The cell system temperature was kept constant at 37 °C throughout the experiment by recirculating water from a thermostatically controlled bath. Continuous stirring at 200 rpm was provided by stirring bars placed in the receptor compartment. Dissolution experiments were conducted spreading the powder directly on the membrane. The receptor compartment was filled with 7 ml of a phosphate-buffered saline (PBS) and isopropyl alcohol in a 7/3 ratio (pH 6.8). This solvent was selected after several preliminary studies, aimed to maintain the sink conditions throughout the experiment. The pH value was raised to around 6.8 because lung lining fluid is often considered almost neutral, but several studies have suggested that it can change depending on circumstances, such as when an inflammatory state is present [11]. A nitrocellulose membrane (size pores: 0.45 μm) was applied between the two compartments (permeation area 1.77 cm^2). About 20 mg of the selected powder, precisely weighed, were uniformly dusted on the membrane surface in the dosage wafer. Samples (500 μl) were removed at defined time intervals (15, 30, 45, 60, 90, 120, 150, 180, 240, 300 and 360 min) inserting the same volume of warmed buffer. Nintedanib was quantified by UV detection (Evolution 201, Thermo Fisher Scientific, Spectral, Ozzano dell'Emilia, Bologna, Italy) at a wavelength of 389 nm. The amount of the drug permeated per area (Q) for each time interval was calculated by means of the following equation:

$$Q\left(mg \,/\, cm^2\right) = \frac{V_R \; x \; C_n + \sum_{i=1}^{n=1} V_P \; x \; C_i}{A}$$

where, VR is the receiver volume; Cn is the drug concentration in the receiver at the time n; VP is the volume of the removed sample Ci is the drug concentration in the receiver at the time n − 1; A is the permeation area (cm^2).

3. Results and discussions

3.1. Feed composition

As to feed preparation, to solve the problems related to the drug's poor solubility in water (11.98 μg•mL^{-1} at pH 6.8 PBS and 5.13 μg•mL^{-1} at pH 7.4 PBS) [12], a hydroalcoholic solution was used and few drops of 1 M HCl solution (pH = 6 ± 0.5) were added with the aim to exploit the molecule pH-dependent solubility. Initially, the hydroalcoholic solution consisted of water/ethanol 7/3 v/v, but the powders obtained presented large crystals as evidenced by morphological analysis (Fig. 1), requiring a change of the hydroalcoholic solution. Therefore, a different alcohol, isopropyl alcohol (from 30 % to 50 % v/v), was used which showed greater solvent power. No further studies were carried out with ethanol: its increase, in fact, is linked to an increase in production costs, as well as an increased risk of flammability, without remarkable improvement of the particles properties (data not shown).

Initially, drug-only powders were produced: to this purpose a 3–4 % w/v concentration was selected: based on our previous experiences [13, 14], these concentrations allow us to obtain powders with a good compromise between particles diameter suitable for inhalation and acceptable process yield. However, the obtained products were
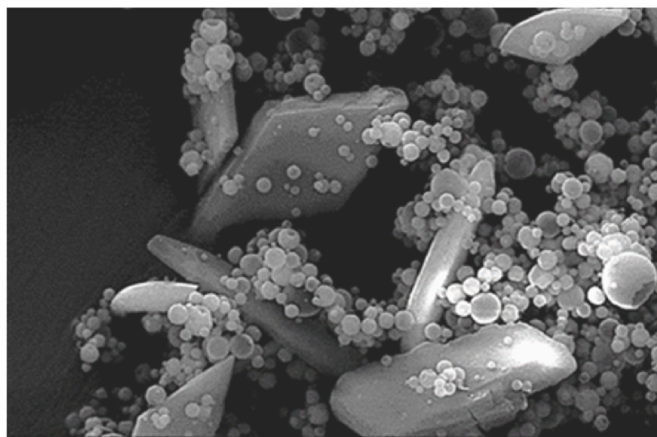

Fig. 1. SEM imagine of particles dried from water/ethanol 7/3 v/v solution.

particularly sticky and electrostatic, making subsequent analysis difficult to carry out. Therefore, suitable excipients were used. Currently, excipients approved for respiratory drug delivery are restricted in number [15]. The array of potential excipients is limited to compounds that are biocompatible or endogenous to the lung and can easily be metabolized or cleared [16].

Among potential excipients, span85 and lecithin were selected and added separately to the feed solutions to reduce the electrostaticity of powders from the FDA's list of GRAS. Span85 is a non-ionic surfactant, while lecithin is an amphoteric surfactant commonly used in the pharmaceutical industry.

L-leucine was used thanks to its well know positive effect on the dispersibility of fine particles [17]. It is a weak surfactant, with a predominantly hydrophobic character. During the drying process, this amino acid tends to migrate and accumulate on the surface of the droplets with the hydrophobic portion directed externally. Moreover, its low solubility facilitates its supersaturation and precipitation on the droplet surface at the beginning of spray drying by forming a hydrophobic shell that may prevent humidity penetration [18].

3.2. Dry powders production and characterization

As reported in Table 2, process yields are generally good for all batches produced regardless of composition but the most important effect was obtained with L-leucine: this excipient in fact generally improved the performance of the process up to about 80 % yield value for Niniso5_leu5 dried from 6/4 water/isopropyl alcohol ratio solution: the creation of a hydrophobic layer on the surface of the particles, indeed, reduced their adhesiveness, preventing the loss of product on the walls of the chamber and the cyclone of the spray. Although the powders obtained using span85 and lecithin showed a reduction in electrostaticity, these excipients were not efficient in decreasing adhesiveness and consequently they were no longer investigated.

Results regarding particle diameters and size distribution were reported as d$_{50}$ and SPAN (Table 2). Generally, the geometric diameter (d$_{50}$) for all batches is suitable for inhalation regardless of composition, ranging between 1.7 and 3.4.

However, some consideration can be done on SPAN values: The batches containing only drugs, regardless of the amount of alcohol (Niniso3, Niniso4 and Niniso5) showed a size distribution with a bimodal trend (Fig. 2, A) due to the formation of particle aggregates with consequent high SPAN values (Table 2). Aggregates formation was not resolved with the use of span85 and lecithin: these excipients also showed a bimodal size distribution curve (Fig. 2, B), while better results were obtained by adding leucine to the feed.

Leucine's dispersibility enhancer effect resulted in a unimodal size distribution curve (Fig. 2, C) and SPAN value closer to 1 when an

Table 2
Spray yield and size distribution of spray-dried powders.

BATCH	YIELD (%)	d_{50} (µm) and (SPAN)	BATCH	YIELD (%)	d_{50} (µm) and (SPAN)
Niniso3	62.3	1.72 (8.72)	**Niniso4_leu7.5**	75.5	1.77 (1.56)
Niniso3	66.8 ± 1.3	2.36 (10.34)	**Niniso4_leu5**	70.7	1.98 (1.70)
Niniso4	66.3	1.80 (4.78)	**Niniso4_leu5**	74.9 ± 1.1	1.86 ± 0.01 (1.70 ± 0.20)
Niniso4	76.5	1.69 (2.10)	**Niniso4_leu2.5**	72.6	1.70 (3.31)
Niniso5	70.6	1.97 (5.36)	**Niniso5_leu10**	78.9	2.48 (2.13)
Niniso4_S85	54.6	2.68 (10.37)	**Niniso5_leu5**	79.6 ± 1.5	2.13 ± 0.05 (1.92 ± 0.01)
Niniso4_le	65.3	3.43 (10.45)	**Niniso5_leu5**	77.5 ± 1.3	2.00 ± 0.02 (1.72 ± 0.11)
Niniso4_leu10	78.5	2.24 (1.89)			

*Relative amount of excipient by % in weight compared to the total amount of dry substance.

excipient concentration higher than 2.5 % w/w was used, since a lower concentration was not sufficient for an adequate dispersion of particles, not preventing the formation of agglomerations. This was also confirmed by the SPAN value of 3.31.

Considering the aerodynamic diameter formula (Eq. 1):

$$d_{ae} = d_v \left(\frac{\rho}{\rho_0 \chi} \right)^{1/2} \tag{1}$$

the aerodynamic properties of a powder depend on particle shape (χ) observed by means of SEM analysis besides volume diameter (Dv) and density (ρ). In particular, the shape factor is defined as the ratio of the drag force on a particle to the drag force on a volume-equivalent sphere at the same velocity. An increase in particle surface roughness corresponds to an increase in shape factor and a consequent decrease in the aerodynamic diameter [19].

Batches processed with only drug are characterized by a smooth and spherical surface. As the amount of drug increases, however, these characteristics tend to decrease. Probably this condition could be related to the lower amount of liquid to evaporate, with a consequent increase in the drying speed that did not allow the movement of solids towards the center of the particle.

In contrast, particles in which leucine is present appear more corrugated: the morphology, indeed, is strongly influenced by the solubility of the components and their initial saturation in the feed. Components that are poorly soluble in water, such as leucine, reach their solubility limit faster, resulting in the precipitation of leucine on the droplet surface at the beginning of the drying process [6].

Whether a compound enriches at the surface during the spray-drying process and to what extent is described by the Peclet number (Eq. (2)). A Peclet number above one results in surface enrichment [6,20].

$$\text{Peclet: } Pe = k/8D \tag{2}$$

where k is the evaporation rate constant in $cm^2\ s^{-1}$ and D is the diffusion coefficient of dissolved substance in the solution.

The evaporation rate varies depending on the atomization parameters and the composition of the feed liquid. A higher inlet temperature of the spray dryer induces a faster evaporation rate, hence a higher Pe number. In addition, the solubility and concentration of feed components can change the evaporation rate. More hydrophobic excipients, for example, tend to have a higher Pe number due to higher evaporation rates and consequently enrich the particle surface [17].

Diffusion velocity, on the other hand, refers to the speed at which molecules or solid particles are transported through the droplet. In the case of leucine, the diffusion velocity during drying tends to decrease due to its low solubility in water ($Pe > 1$), reaching a supersaturated condition more quickly, resulting in precipitation of the leucine on the surface of the droplet. This leads to the formation of a hydrophobic layer that interferes with water diffusion and induces the formation of corrugated particles [21](Fig. 3, C; D; E and F). The addition of a further 5 % leucine into the liquid feed (Fig. 3C and D) led to a precipitation of the leucine in small crystals generating a cobweb effect all around the
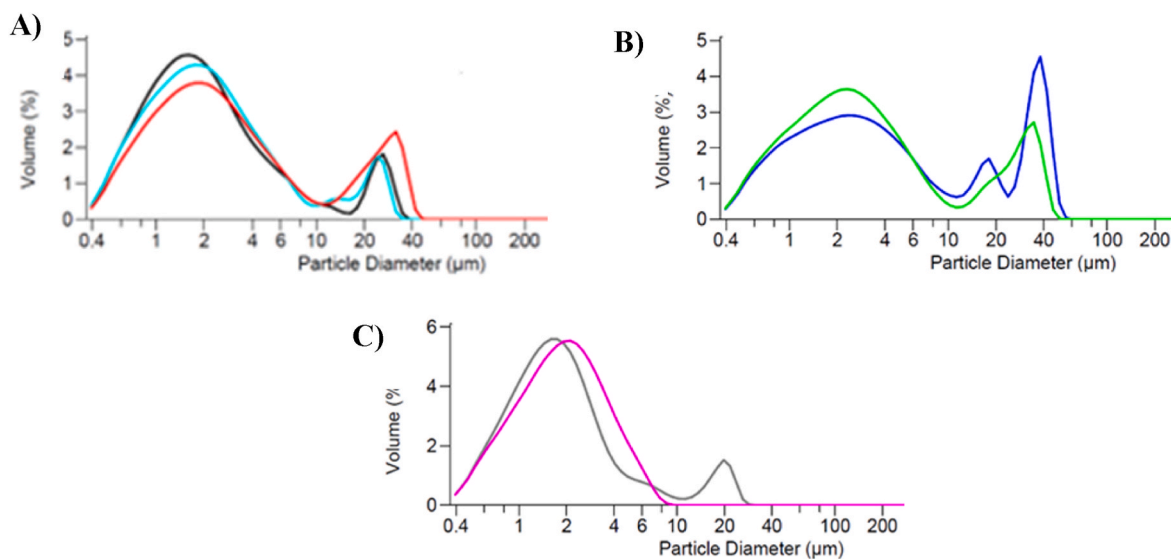

Fig. 2. Size distribution of **A**, Niniso3 (red), Niniso4 (black) and Niniso5 (azure) dried from 6/4 water/isopropyl alcohol ratio solution; **B**, Niniso4_S85 (green) and Niniso4_le (blue); **C**, Niniso5_leu5 (pink) and Niniso4_leu2.5 (grey) dried from 6/4 water/isopropyl alcohol ratio solution. (For interpretation of the references to color in this figure legend, the reader is referred to the Web version of this article.)

particles, indicating an excessive amount of excipient, as clearly visible in Fig. 3C.

The density of the batches produced was also evaluated. From the data shown in Table 3, bulk (ρ_b) and tapped (ρ_t) density increased in batches containing leucine, compared to reference batches of only drug, regardless of the concentration. The density is also a function of the behavior of the particles during packing; in the specific case of powders characterized by a smaller size and a corrugated surface, during the packing the space between the particles decreases, which leads to an increase in density. High density values can have a negative impact on aerodynamic properties; however, a higher density allows more powder to be loaded into the capsules.

Poor particle flowability results in high retention in the capsule, in the device and in the upper part of the impactor during the *in vitro* inhalation study. Therefore, satisfactory particle flowability is one of the main prerequisites for high aerosolization performance. The bulk (ρ_b) and tapped (ρ_t) densities of different powder formulations were measured to calculate Carr's Index which are closely associated with interparticle interactions. Lower values of Carr's Index indicate less cohesiveness and better flowability of powders [5].

Table 3 shows that the drug-only batches were characterized by the highest Carr's Index values (up to 56 %), whereas, the addition of 5 % leucine was sufficient to have a significant reduction of this value regardless of the composition of the hydroalcoholic solution (Niniso4_leu5 and Niniso5_leu5); further additions of leucine did not lead to a further reduction of the Carr's Index (Niniso4_leu7.5, Niniso4_leu10 and Niniso5_leu10), indicating that the amino acid was already sufficiently distributed on the surface of the particles. Less important improvement was found for the baches Niniso4_S85 (66 %) and Niniso4_le (58 %).

The DSC thermograms of raw materials, which did not undergo the spray-drying process, showed a melting peak at 260 °C for Nintedanib and at around 315 °C for leucine (Fig. 4). The curves corresponding to the batches processed with only 4 % w/v drug, and that with 5 % w/w leucine added at the same drug concentration (4 %) showed the typical behavior of amorphous material with an initial loss of water, followed by the presence of an exothermic peak due to the recrystallisation of the drug at around 200 °C. The spray treatment therefore induces batch amorphization and this is confirmed by Powder X-ray Diffraction (PXRD) (Specific details are provided in Supplementary Materials). Subsequently, the presence of a melting peak was observed and finally the degradation of the drug. Fig. 4 shows the thermogram of only one batch containing leucine as all the others, characterized by the presence

Table 3
Bulk and tapped density and Carr's Index.

BATCH	H$_2$O/2-PrOH (v/v)	ρ_b (mg/mL)	ρ_t (mg/mL)	Carr's Index (%)
Niniso3	7/3	127.1 ± 9.3	297.8 ± 2.5	57.3 ± 3.1
Niniso3	6/4	109.4 ± 2.6	249.9 ± 21.0	56.0 ± 3.9
Niniso4	6/4	95.7 ± 1.8	305.8 ± 10.8	68.7 ± 1.2
Niniso4	5/5	128.6 ± 5.7	301.8 ± 8.1	57.3 ± 3.1
Niniso5	6/4	105.7 ± 2.0	284.2 ± 18.4	62.0 ± 0.2
Niniso4_S85	6/4	92.7 ± 4.9	272.7 ± 14.4	61.0 ± 0.1
Niniso4_le	6/4	143.7 ± 7.5	342.2 ± 13.9	58.0 ± 0.1
Niniso4_leu10	6/4	159.9 ± 1.5	361.2 ± 0.3	47.0 ± 0.0
Niniso4_leu7.5	5/5	286.9 ± 3.5	486.5 ± 17.7	40.7 ± 1.2
Niniso4_leu5	6/4	154.1 ± 8.4	340.9 ± 29.6	44.1 ± 0.1
Niniso4_leu5	5/5	267.6 ± 11.5	456.0 ± 10.7	41.3 ± 1.2
Niniso4_leu2.5	5/5	145.6 ± 7.3	325.9 ± 14.1	49.5 ± 1.1
Niniso5_leu10	6/4	199.2 ± 0.8	383.1 ± 16.5	48.2 ± 0.1
Niniso5_leu5	6/4	240.9 ± 14.1	469.3 ± 20.7	46.1 ± 0.1
Niniso5_leu5	5/5	279.7 ± 8.5	482.3 ± 13.1	44.2 ± 2.8

of the same excipient, had a similar trend.

The results of the thermogravimetric analysis (TGA) of the spray-dried powders (Niniso 4 and Niniso4_leu5 dried from 5/5 water/iso-propyl alcohol ratio) after production and after one year storage at room conditions, evidenced almost no change in water content for batches containing leucine (from 6.5%w/w to 5.9%w/w) and a slight increase in water content for only-drug powders (from 3.9 % w/w to 4.8 % w/w).

3.3. In vitro aerosolization performance

The results reported in Table 4 indicated that the emitted dose for all batches, using the Single Stage Glass Impinger, was greater than 93 % of the charged formulation, demonstrating a very efficient disaggregation of powders by means of the selected device. Despite the overall
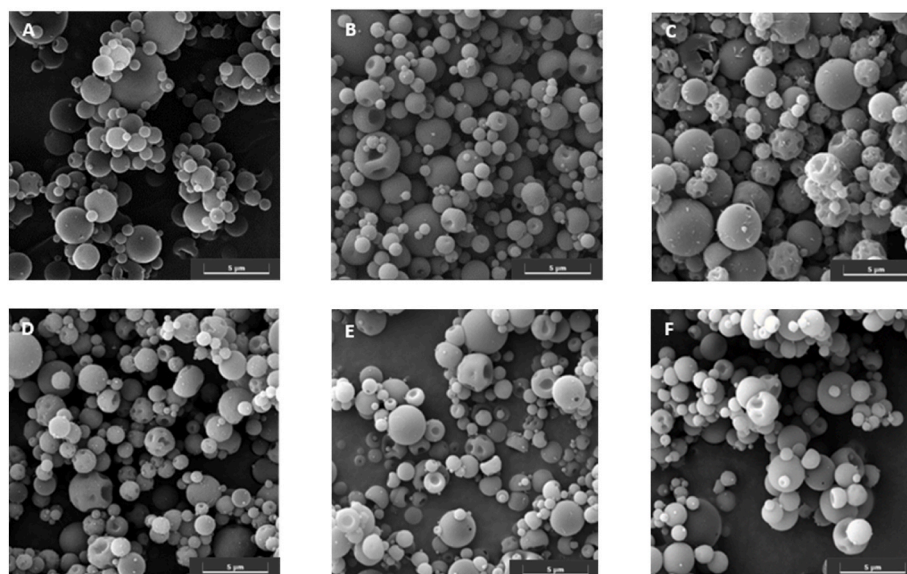

Fig. 3. SEM images of A, Niniso4; B, Niniso5; C, Niniso4_leu10; D, Niniso4_leu7.5; E, Niniso4_leu5; F, Niniso4_leu2.5.
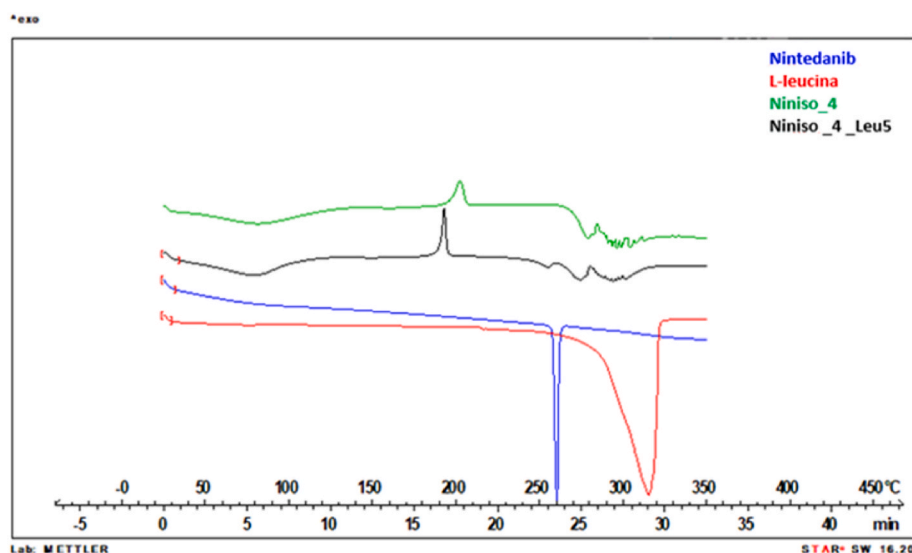
Fig. 4. Differential scanning calorimetry thermograms of Nintedanib (blue), L-leucine (red), Niniso4 (green) and Niniso4_Leu5 dried from 5/5 water/isopropyl alcohol ratio (black). (For interpretation of the references to color in this figure legend, the reader is referred to the Web version of this article.)

Table 4
Aerodynamic properties of powders using Single Stage Glass Impinger.

BATCH	H$_2$O/2-PrOH (v/v)	ED (%)	FPF (%)
Niniso3	7/3	99.1 ± 1.6	31.0
Niniso3	6/4	98.2 ± 1.5	24.7 ± 0.1
Niniso4	6/4	95.8 ± 1.6	41.1 ± 12.1
Niniso4	5/5	99.9 ± 1.2	47.9 ± 5.4
Niniso5	6/4	98.1 ± 0.9	36.8
Niniso4_S85	6/4	99.9 ± 1.1	61.6
Niniso4_le	6/4	93.2 ± 11.8	50.9
Niniso4_leu10	6/4	99.1 ± 0.5	73.5
Niniso4_leu7.5	5/5	99.3 ± 0.7	71.6
Niniso4_leu5	6/4	95.4 ± 2.9	64.01
Niniso4_leu5	5/5	99.4 ± 0.6	72.1 ± 1.3
Niniso4_leu2.5	5/5	93.5 ± 2.3	47.0 ± 5.3
Niniso5_leu10	6/4	98.9 ± 0.6	62.4
Niniso5_leu5	6/4	99.0 ± 0.8	68.9 ± 2.6
Niniso5_leu5	5/5	99.8 ± 0.7	72.3 ± 1.8

satisfying values of ED, the highest fine particle fraction (FPF) values were obtained for batches in which the amino acid was present. Due to its ability to reduce inter-particle interaction forces, typical of particles with irregular surfaces, leucine prevented particle agglomeration.

MMAD and FPF values derived by ACI deposition studies for the Niniso4 and Niniso4_ leu5 batches dried from 5/5 water/isopropyl alcohol ratio, confirmed the observed leucine concentration-dependent trends (Table 5). For inhalation into the lower airways and into the deep lung, a better dispersibility of particles with MMAD <5 μm is a prerequisite.

As shown in Fig. 5, a 5 % leucine addition to the liquid feeds led to an

Table 5
Aerodynamic properties of powders using ACI.

BATCH	H$_2$O/2-PrOH (v/v)	MMAD	ED (%)	FPF (%)	Flow rate (L/min)
Niniso4	5/5	3.56 ± 0.9	98.2 ± 0.3	56.5 ± 4.4	60
Niniso4_leu5	5/5	2.66 ± 0.3	100.9 ± 0.1	79.1 ± 1.2	60
Niniso4	5/5	4.04 ± 0.1	99.86 ± 0.5	51.5 ± 1.0	30
Niniso4_leu5	5/5	2.23 ± 0.4	104.5 ± 1.6	77.6 ± 2.5	30

increase in FPF with a reduction in the undesirable powder deposition in the throat. This occurred both at a flow rate of 60 L/min and of 30 L/min.

Generally, the flow rate is a crucial parameter that can influence the dispersion of drug particles and their deposition in the lungs. A reduction in flow rate can induce a decrease in the speed of drug particles during inhalation compromising their ability to overcome device resistance and reach deep regions of the lungs. In addition, a lower flow rate may result in insufficient dispersion of the particles and a less uniform distribution in the aerosol, affecting the amount of drug available for deposition in the lungs. In the case of Nintedanib microparticles, however, the reduction of the flow rate did not influenced their aerodynamic performance, in particular with leucine containing powders.

3.4. UHPLC-PDA and LCMS/MS profiles of standard nintedanib and spray-dried formulations

Appropriate studies were carried out to verify that the acid treatment and drying process had no negative effect on the molecule structural integrity. To the best of our knowledge, this is the first work to report such studies applied to the Nintedanib. The UHPLC-PDA profile of the spray-dried formulation (Niniso4 dried from 6/4 water/isopropyl alcohol ratio solution) revealed the presence of a single chromatographic peak with a retention time of 8.5 min (Fig. 6, B), which matched the standard Nintedanib (Fig. 6, A). This suggests that the formulation process did not cause any significant changes to the chemical integrity of the active pharmaceutical ingredient (API). To further confirm the chemical integrity of the molecule after the spray drying process, LC-MS/MS analysis was performed using electrospray ionization (ESI) in positive ionization mode. The mass spectrum showed a precursor ion peak at m/z 540.2606 [M − H]+, corresponding to the molecular weight of the Nintedanib (Fig. 6C and D). The fragmentation pattern of the precursor ion provides additional structural information about the compound. The MS/MS fragments observed at m/z 113 ($C_6H_{13}N_2$), m/z 483 ($C_{28}H_{27}O_4N_4$) and m/z 141 ($C_7H_{13}ON_2$) correspond to specific fragments of the Nintedanib [22]. Overall, the presence of the chromatographic peak with the same retention time as the standard NTB, as well as the matching mass spectrum and MS/MS fragments, provides strong evidence that the API maintained its chemical integrity throughout the spray-drying formulation process.
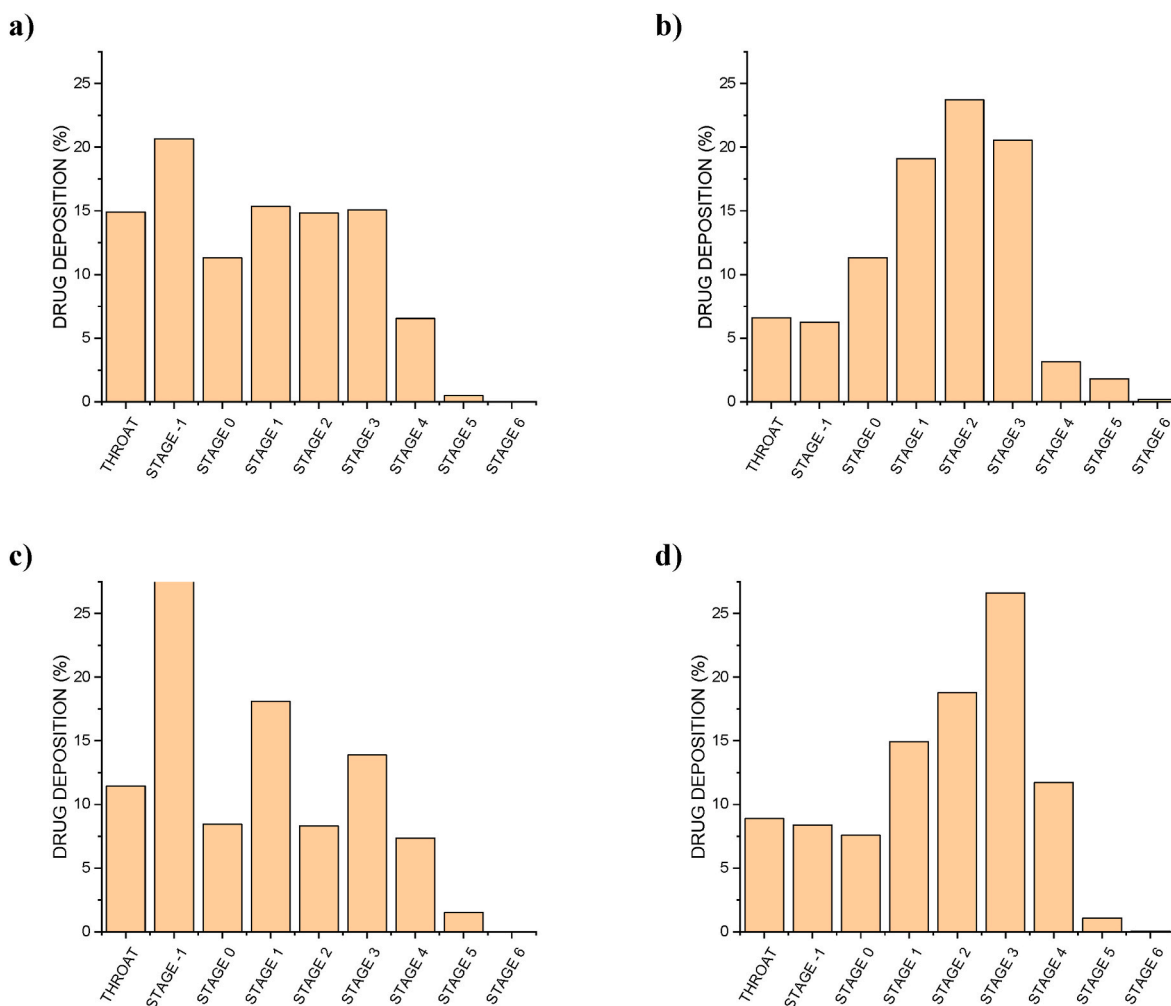
Fig. 5. Andersen cascade impact deposition scheme of a) Niniso4, b) Niniso4_leu5, both with a flow rate of 60 L/min and c) Niniso4, d) Niniso4_leu5 both with a flow rate of 30 L/min.

3.5. *In vitro dissolution by Franz cell method*

In the context of dry powder formulations, the dissolution of drug particles deposited on airway surfaces plays a key role in ensuring efficacy. Dissolution is also hindered by the lung surface, which does not provide ideal conditions for this to occur due to limited fluid volume and particle elimination mechanisms. Furthermore, for drugs that are poorly soluble in water, such as Nintedanib, it is critical to enhance dissolution and maintain drug concentrations in the lung lining fluid above minimum inhibitory concentrations [23–25]. In this work, dissolution studies were conducted through the Franz cell method. The As shown in Fig. 7, the dissolution rate of the spray-dried formulation containing only the drug (Niniso4 dried from 5/5 water/isopropyl alcohol ratio) reaches approximately 4 % during the initial dissolution phase (within the first 15 min). In contrast, there is a significant increase in the dissolution rate in the presence of 5 % leucine (Niniso4_leu5 dried from 5/5 water/isopropyl alcohol ratio), which reaches about 10 % during the same time interval.

4. Conclusion

The fine tuning of spray drying process parameters, together with the selection of opportune excipients allowed to obtain nintedanib powders with well-defined technological properties. The best micronized particles in terms of yield, flowability, SPAN, morphology and aerodynamic performance were those in which leucine was present: in particular an excipient concentration of 2.5 % proved insufficient to avoid particles agglomeration, while a concentration of 10 % determined the precipitation of the excipient on the surface of the particles in the form of fine crystals with a cobweb effect evidenced by SEM analysis. The encouraging results shown in this work, make the Nintedanib based DPI a very promising product for the management of pulmonary fibrosis representing an advantageous alternative to traditional routes of administration reducing, in fact, the systemic exposure to the drug and, consequently, its side effects.

CRediT authorship contribution statement

Valentina Ruggiero: Investigation, Writing – original draft, Writing – review & editing. **Giovanna Aquino:** Formal analysis, Investigation. **Pasquale Del Gaudio:** Visualization, Writing – review & editing. **Teresa Mencherini:** Conceptualization, Formal analysis. **Consiglia Tedesco:** Data curation, Formal analysis. **Paola Russo:** Funding acquisition, Supervision, Writing – original draft, Writing – review & editing.
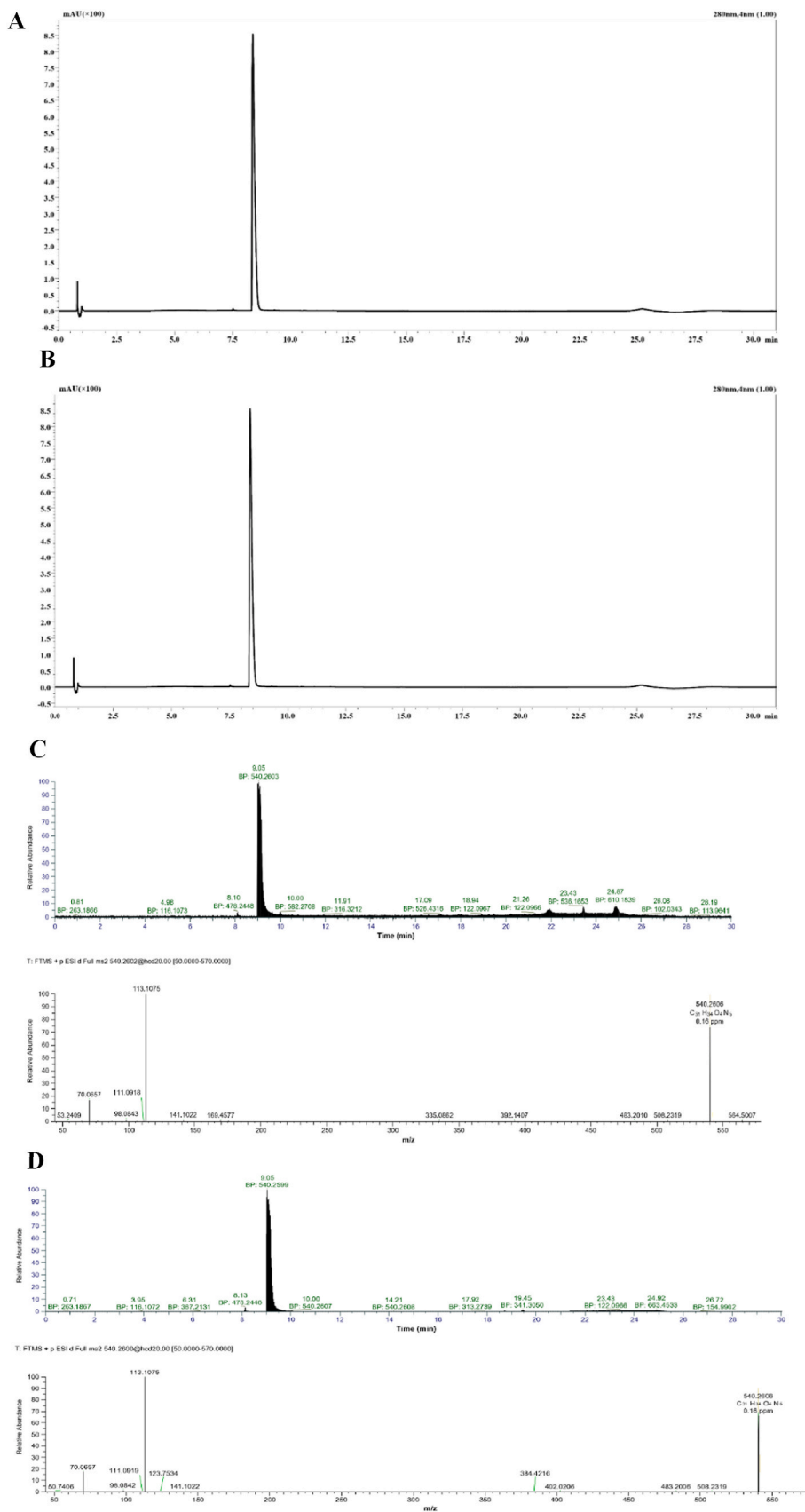
Declaration of competing interest

Fig. 6. UHPLC-PDA profiles of A, Nintedanib and B, Niniso4 dried from 6/4 water/isopropyl alcohol ratio solution. LCMS/MS profiles of C, Nintedanib and D, Niniso4 dried from 6/4 water/isopropyl alcohol ratio solution.
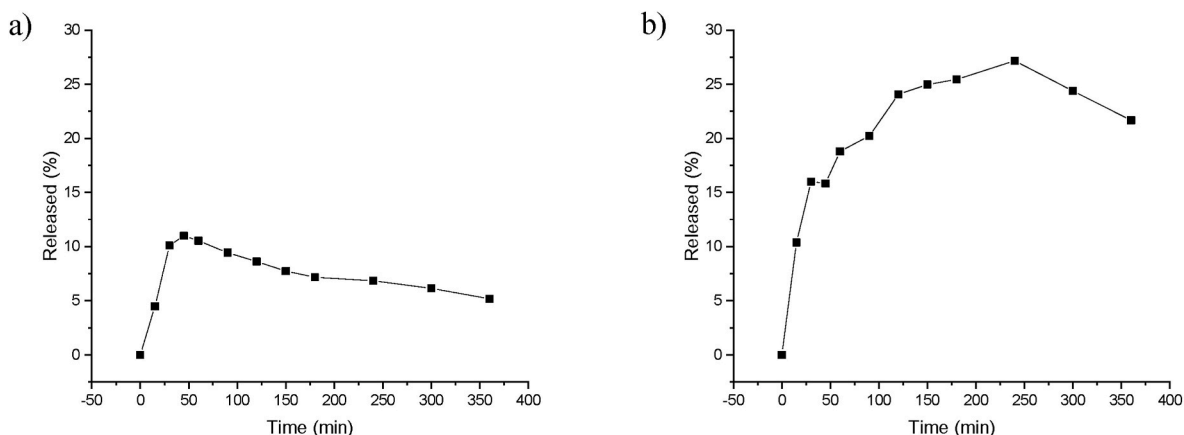
Fig. 7. In vitro dissolution of a) Niniso4 dried from 5/5 water/isopropyl alcohol ratio and b) Niniso4_leu5 dried from 5/5 water/isopropyl alcohol ratio.

Data availability

Data will be made available on request.

Acknowledgements

Appendix A. Supplementary data

Supplementary data to this article can be found online at https://doi.org/10.1016/j.jddst.2024.105340.

References

[1] M.C. Volpe, G. Ciucci, G. Zandomenego, R. Vuerich, N.A.R. Ring, S. Vodret, F. Salton, P. Marchesan, L. Braga, T. Marcuzzo, R. Bussani, A. Colliva, S. Piazza, M. Confalonieri, S. Zacchigna, Flt1 produced by lung endothelial cells impairs ATII cell transdifferentiation and repair in pulmonary fibrosis, Cell Death Dis. 14 (2023) 437.

[2] J. Hutchinson, A. Fogarty, R. Hubbard, T. McKeever, Global incidence and mortality of idiopathic pulmonary fibrosis: a systematic review, Eur. Respir. J. 46 (2015) 795–806.

[3] L. Wollin, E. Wex, A. Pautsch, G. Schnapp, K.E. Hostettler, S. Stowasser, M. Kolb, Mode of action of nintedanib in the treatment of idiopathic pulmonary fibrosis, Eur. Respir. J. 45 (2015) 1434–1445.

[4] P.M. George, A.U. Wells, R.G. Jenkins, Pulmonary fibrosis and COVID-19: the potential role for antifibrotic therapy, Lancet Respir. Med. 8 (2020) 807–815.

[5] X. Wang, W. Wan, J. Lu, G. Quan, X. Pan, P. Liu, Effects of L-leucine on the properties of spray-dried swellable microparticles with wrinkled surfaces for inhalation therapy of pulmonary fibrosis, Int. J. Pharm. 610 (2021) 121223.

[6] R. Vehring, Pharmaceutical particle engineering via spray drying, Pharm. Res. (N. Y.) 25 (2008) 999–1022.

[7] M.L. Stewart, J.L. Slavin, Particle size and fraction of wheat bran influence short-chain fatty acid production in vitro, Br. J. Nutr. 102 (2009) 1404–1407.

[8] P. Del Gaudio, G. Auriemma, P. Russo, T. Mencherini, P. Campiglia, M. Stigliani, R. P. Aquino, Novel co-axial prilling technique for the development of core–shell particles as delayed drug delivery systems, Eur. J. Pharm. Biopharm. 87 (2014) 541–547.

[9] F. Sansone, R.P. Aquino, P. Del Gaudio, P. Colombo, P. Russo, Physical characteristics and aerosol performance of naringin dry powders for pulmonary delivery prepared by spray-drying, Eur. J. Pharm. Biopharm. 72 (2009) 206–213.

[10] R.J. Panos, R.L. Mortenson, S.A. Niccoli, T.E. King Jr., Clinical deterioration in patients with idiopathic pulmonary fibrosis: causes and assessment, Am. J. Med. 88 (1990) 396–404.

[11] A.W. Ng, A. Bidani, T.A. Heming, Innate host defense of the lung: effects of lung-lining fluid pH, Lung 182 (2004) 297–317.

[12] H. Liu, J. Mei, Y. Xu, L. Tang, D. Chen, Y. Zhu, S. Huang, T.J. Webster, H. Ding, Improving the oral absorption of nintedanib by A self-microemulsion drug delivery system: preparation and in vitro/in vivo evaluation, Int. J. Nanomed. 14 (2019) 8739–8751.

[13] M.D. Manniello, P. Del Gaudio, R.P. Aquino, P. Russo, Clarithromycin and N-acetylcysteine co-spray-dried powders for pulmonary drug delivery: a focus on drug solubility, Int. J. Pharm. 533 (2017) 463–469.

[14] M. Stigliani, R.P. Aquino, P. Del Gaudio, T. Mencherini, F. Sansone, P. Russo, Non-steroidal anti-inflammatory drug for pulmonary administration: design and investigation of ketoprofen lysinate fine dry powders, Int. J. Pharm. 448 (2013) 198–204.

[15] G. Pilcer, K. Amighi, Formulation strategy and use of excipients in pulmonary drug delivery, Int. J. Pharm. 392 (2010) 1–19.

[16] D. Zillen, M. Beugeling, W.L.J. Hinrichs, H.W. Frijlink, F. Grasmeijer, Natural and bioinspired excipients for dry powder inhalation formulations, Curr. Opin. Colloid Interface Sci. 56 (2021) 101497.

[17] A. Lechanteur, B. Evrard, Influence of composition and spray-drying process parameters on carrier-free DPI properties and behaviors in the lung: a review, Pharmaceutics 12 (2020).

[18] L. Li, S. Sun, T. Parumasivam, J.A. Denman, T. Gengenbach, P. Tang, S. Mao, H. K. Chan, L-Leucine as an excipient against moisture on in vitro aerosolization performances of highly hygroscopic spray-dried powders, Eur. J. Pharm. Biopharm. 102 (2016) 132–141.

[19] M. Stigliani, R.P. Aquino, P. Del Gaudio, T. Mencherini, F. Sansone, P. Russo, Non-steroidal anti-inflammatory drug for pulmonary administration: design and investigation of ketoprofen lysinate fine dry powders, Int. J. Pharm. 448 (2013) 198–204.

[20] I. Sibum, P. Hagedoorn, M.P.G. Kluitman, M. Kloezen, H.W. Frijlink, F. Grasmeijer, Dispersibility and storage stability optimization of high dose isoniazid dry powder inhalation formulations with L-leucine or trileucine, Pharmaceutics 12 (2019).

[21] S. Focaroli, P.T. Mah, J.E. Hastedt, I. Gitlin, S. Oscarson, J.V. Fahy, A.M. Healy, A Design of Experiment (DoE) approach to optimise spray drying process conditions for the production of trehalose/leucine formulations with application in pulmonary delivery, Int. J. Pharm. 562 (2019) 228–240.

[22] D. Lin, L.M. Qiao, Y.N. Zhang, Y. Liu, X.S. Liu, Simultaneous determination of nintedanib and its metabolite by UPLC-MS/MS in rat plasma and its application to a pharmacokinetic study, J. Pharm. Biomed. Anal. 117 (2016) 173–177.

[23] C. Duret, N. Wauthoz, T. Sebti, F. Vanderbist, K. Amighi, Solid dispersions of itraconazole for inhalation with enhanced dissolution, solubility and dispersion properties, Int. J. Pharm. 428 (2012) 103–113.

[24] S. Mangal, H. Nie, R. Xu, R. Guo, A. Cavallaro, D. Zemlyanov, Q.T. Zhou, Physico-chemical properties, aerosolization and dissolution of Co-spray dried azithromycin particles with L-leucine for inhalation, Pharm. Res. (N. Y.) 35 (2018) 28.

[25] S.I. Rennard, G. Basset, D. Lecossier, K.M. O'Donnell, P. Pinkston, P.G. Martin, R. G. Crystal, Estimation of volume of epithelial lining fluid recovered by lavage using urea as marker of dilution, J. Appl. Physiol. 60 (1986) 532–538.